

6B.3 SYNOPTIC COMPOSITES OF THE EXTRATROPICAL TRANSITION LIFECYCLE OF NORTH ATLANTIC TROPICAL CYCLONES: FACTORS DETERMINING POST-TRANSITION EVOLUTION

Robert E. Hart¹, Jenni L. Evans², and Clark Evans¹

¹Department of Meteorology, Florida State University

²Department of Meteorology, Pennsylvania State University

1. INTRODUCTION

Over the past five years, the extratropical transition (ET) lifecycle has been defined based upon satellite signatures (Klein et al. 2000) and objective measures of dynamic and thermal structure (Evans and Hart 2003). Following ET, tropical cyclones (TCs) can become explosive cold-core cyclones, explosive warm-seclusion cyclones, or simply decay as a cold-core cyclone (Hart 2003; Evans and Hart 2003). Each of these three evolution paths has dramatically different wind and precipitation field (Bosart et al. 2001), and ocean wave (Bowyer 2000; Bowyer and Fogarty 2003) responses associated with it. Furthermore, the envelope of realized intensity is fundamentally related to the structure obtained after ET (Hart 2003), so incorrect forecasts of storm structure have the effect of also degrading the intensity forecasts. Yet, numerical models currently struggle in forecasting the basic nature of TC evolution during and after ET (McTaggart-Cowan et al. 2001; Ma et al. 2003). Indeed, the predictability of the long-wave pattern of the northern hemisphere often becomes unusually low when an ET event is upcoming (Jones et al. 2003a,b).

The goal of the research presented here is to define and distinguish the precursor environments that lead to cases of post-ET weakening, strengthening, and/or cold-core evolution or warm-seclusion. The approach is to normalize the TC lifecycles of each of these 34 cases using the cyclone phase space (CPS; Hart 2003) characterization of cyclone structure. This framework not only permits objective diagnosis of the post-transition structure (cold-core or warm-seclusion), but also enables compositing of precursor and subsequent storm environments for similar phase evolutions. This facilitates a detailed examination of the differing nature of underlying interaction between the TC and trough. Further, composites of the precursor environments will provide forecasters with schematics for future cyclone evolution, even in situations of low predictability using the numerical model guidance alone.

2. DATA AND METHODOLOGY

a. Datasets

Storm composites performed here were based upon $1^\circ \times 1^\circ$ resolution Navy Operational Global Atmospheric Prediction System (NOGAPS; Hogan et al. 1991) operational analyses for the period 1998-2003. During these six years, 34 Atlantic TCs underwent resolvable ET as diagnosed within the cyclone phase space (CPS) (<http://moe.met.fsu.edu/cyclonephase>).

b. Methodology

i. Normalizing the ET timeline

The ET lifecycle defined in Evans and Hart (2003) is used here, with the beginning of ET (labeled as T_B) as the time when the storm becomes significantly asymmetric ($B > 10$) and end of ET (labeled as T_E) the time when the lower-tropospheric thermal wind indicates a cold core (i.e. $-V_T^L < 0$). These threshold for beginning and end of transition were confirmed by the objective clustering of transitioning storms in the CPS by Arnott et al. (2004).

To examine the precursor and subsequent synoptic evolution of the cyclones, seven additional times were defined with respect to these two points: T_B-72h , T_B-48h , T_B-24h , T_{MID} [$= \frac{1}{2} (T_B + T_E)$], T_E+24h , T_E+48h , and T_E+72h . This normalizing of the ET time line of each TC enables direct comparison of the evolution of one system to another. While all nine milestones are used to produce a composite mean cyclone phase lifecycle, for purposes of brevity only four of the nine milestones are examined here and illustrated with the synoptic composites: T_B-24h , T_B , T_E , and T_E+24h .

ii. Compositing

For each cyclone, a storm-relative $1^\circ \times 1^\circ$ resolution grid, spanning 91° of longitude and 91° of latitude, was centered over the cyclone center. The NOGAPS-based storm-relative grid was then produced for each of the four ET milestones defined above. After this process was repeated for each of the 34 cyclones, the composite mean storm-relative grid was produced.

*Corresponding author address: Robert Hart, 404 Love Building, Florida State University, Tallahassee, FL 32306-4520. Email: rhart@met.fsu.edu

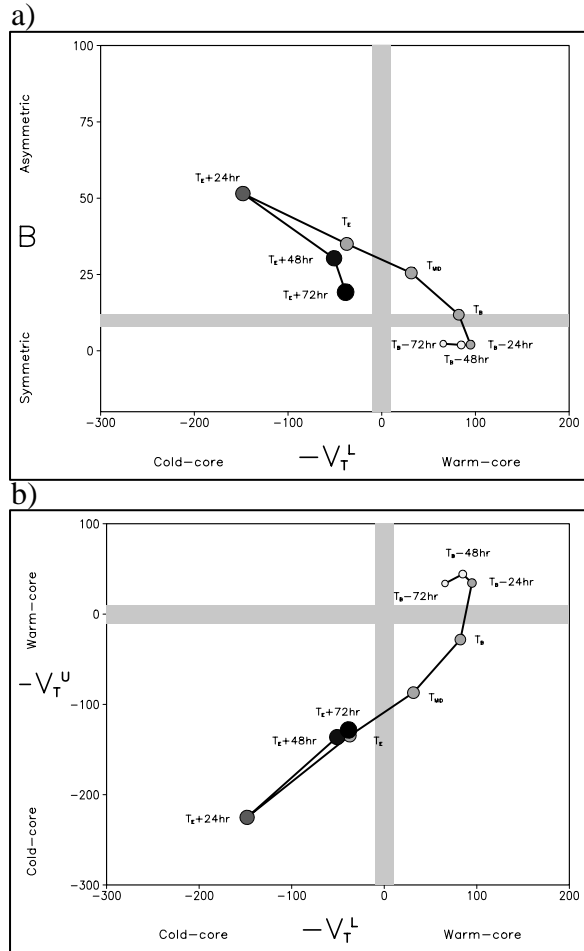


Figure 1: 1998-2003 34-cyclone composite mean cyclone trajectory using NOGAPS 1° analysis. a) B vs. $-V_T^L$ and b) $-V_T^U$ vs. $-V_T^L$. T_B and T_E represent the start and end of ET, respectively, as defined in Evans and Hart (2003), and T_{MID} represents the mid-point of ET. The size of the circular marker indicates the average radius of 925hPa gale force winds, from 225km at T_B-72h to 570km at T_E+72h . The gray shading of the marker indicates minimum mean sea level pressure, from 1001hPa at T_B-72h to 982hPa at T_E+72h . The numbers of available cases for each of the nine times above are 33, 34, 34, 34, 31, 31, 26, 17, and 11. For reasons of brevity, only four of the milestones will be examined here: T_B-24h , T_B , T_E , and T_E+24h .

3. COMPOSITE MEAN EVOLUTION AND ET VARIABILITY

a. Composite mean cyclone phase evolution

The 34-storm composite mean cyclone phase evolution is depicted in Figure 1. The mean evolution of cyclone structure from symmetric warm-core, to hybrid, to asymmetric cold-core to eventual occlusion is well illustrated. The average transitioning TC peaks in warm-core intensity around 24h prior to the start of ET (T_B-24h with $-V_T^L \approx 100$). This result is consistent with Hart and Evans (2001) and illustrates why a significant percentage of Atlantic TCs are capable of undergoing ET in the first place. Complete dissipation of a TC from peak

intensity generally takes several days yet a TC only has to survive for 24h after weakening from peak intensity to reach a baroclinic environment supporting the commencement of ET.

Within 24h of transition completing (T_E+24h), the North Atlantic cyclone has achieved its largest value of B and also has significantly decreased in pressure (Figure 1). The former suggests that upon completion of ET the mean cyclone has reached the strongest storm-motion-relative temperature gradient it will attain. One to two days after this, the cyclone has continued to intensify and expand considerably in size, with B decreasing as the baroclinic instability is removed. Soon after T_E+72h , the occlusion process has begun (not shown).

b. Composite mean evolution during ET

Prior to the start of transition (T_B-24h), the TC has commenced recurvature, but remains distinct from the midlatitude environment (Figures 2a, 3a). The storm's tropical connection is also evident in the equivalent potential temperature field (not shown). While this connection has weakened by the start of transition, the local minimum of static stability associated with the TC (Figure 4a) serves to enhance the Eady baroclinic growth rate, σ , (Eady 1949; $\sigma = fU_z N^{-1}$) of the environment between the trough and TC. Due to the decreased static stability, the trough is effectively made a more dynamically deep baroclinic system through the introduction of the TC and its environment (Harr et al. 2000). Although not shown, the lifting of the tropopause ahead of the trough by the TC's anticyclone increases the baroclinicity of the upper troposphere, leading to enhancement of the jet streak that is typically found with the trough.

By the end of transition (Figure 5c) the moist, unstable core of the remnant TC has weakened considerably; however, a local maximum of 850hPa equivalent potential temperature at the end of transition (Figure 5c) is consistent with Thorncroft and Jones (2000). The remnant maximum of moisture in the presence of a pressure minimum without a larger maximum of temperature illustrates why equivalent potential temperature alone cannot be used as an indicator of warm vs. cold-core structure in cyclones.

A potential vorticity perspective on the ET lifecycle (Figures 6 and 7) illustrates the approach of the trough while the low-level PV maximum of the TC is maintained. Since the 300hPa static stability of the atmosphere is approximately 20% less immediately surrounding the cyclone than between the cyclone and the approaching trough (dotted contours in Figure 7a,b), the TC introduced an environment at upper levels that enhanced the Eady baroclinic growth rate of the wave (Figure 7). By the

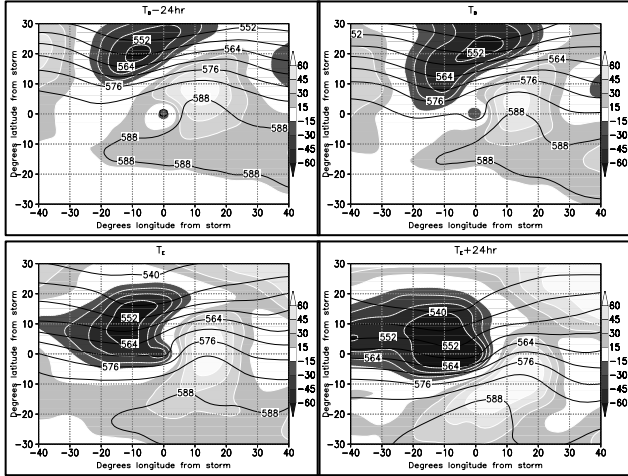


Figure 2: Composite mean 500hPa height (contour, dm) and anomaly from monthly mean (shaded, m) for T_B-24h , T_B , T_E , and T_E+24h . The transitioning storm is located at (0,0) in each panel.

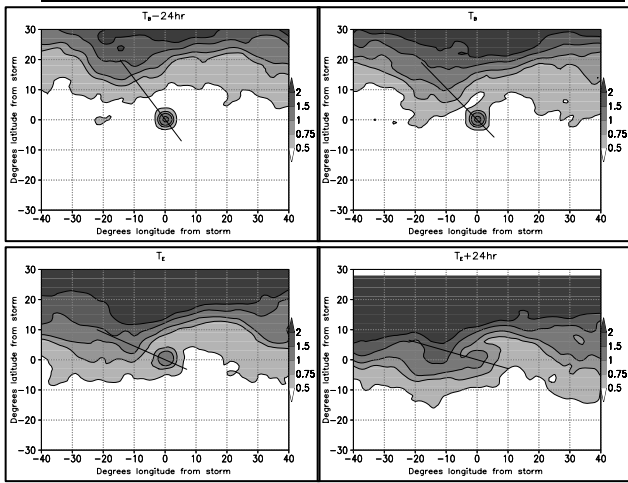


Figure 3: 320K isentropic potential vorticity (shaded, PVU) for a) T_B-24h , b) T_B , c) T_E , and d) T_E+24h . Solid line in each panel is the axis of the cross sections in Figure 4.

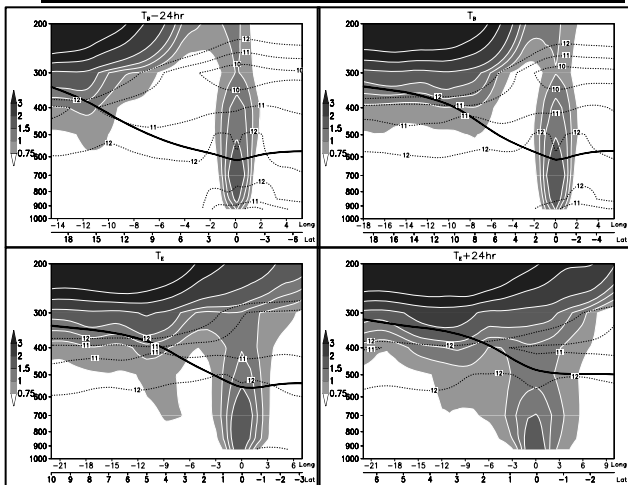


Figure 4: Cross sections (locations shown in Figure 3) of potential vorticity (shaded, PVU), 320K isentropic surface (solid contour), and Brunt-Vaisala frequency (dotted contour, $10^{-2} s^{-1}$) for T_B-24h , T_B , T_E , and T_E+24h .

end of transition (Figure 2c), the TC has interacted with the trough (the nature of which will be discussed next), with the 0.75PVU contour extending below 500hPa by the completion of ET (Figure 4c). By 24h after transition, there is no distinction between the former TC remnant and the trough that interacted with it (Figure 3d).

To illustrate more clearly the trough's forcing upon the TC, the Eliassen-Palm flux analysis in cylindrical-isentropic coordinates of Molinari et al. (1995) and Harr et al. (2000) was performed (Figure 5a-d) using the mean atmospheric state of the 34-cyclone composite for each of the four key ET milestones highlighted here: T_B-24h , T_B , T_E , and T_E+24h . From these analyses, we can determine the relative contribution of the trough in the eddy angular momentum and eddy heat flux forcing (and, implicitly, the eddy potential vorticity flux) within the transitioning TC. Comparisons to the Elena (1985) trough interaction analyses described in Molinari et al. (1995) and the case studies of Harr et al. (2000) can also be drawn.

One day prior to the start of transition (Figure 5a), there is evidence of weak inward eddy angular momentum flux beyond 1000km radius in the middle troposphere, resulting from the approaching trough (Figure 3a). Through ET (Figure 5b,c), the magnitude of eddy angular momentum flux (horizontal vector) increases markedly, leading to an EP flux divergence and inward flux of eddy PV (shading) throughout the entire storm above 315K and between 350km and 1500km radius. Even through T_E , the vast majority of the EP flux divergence is a result of the eddy angular momentum flux rather than the eddy heat flux given the predominant horizontal orientation of the vectors and minimal change in vector magnitude beyond 750km radius. Although requiring more detailed evaluation with numerical modeling, this result suggests that the conversion of the TC from warm core to cold core is predominantly a consequence of the eddy momentum forcing rather than the eddy heat flux. While this may appear paradoxical at first, it is a natural consequence of the timeline of evolution of trough interaction and the trough/TC separation distance throughout. As shown in Figure 3, the TC completes ET (Figure 3c) well before merger (Figure 3d). Given that the majority of the cold air associated with the trough still has not reached the greater part of the storm circulation (not shown), it is not surprising that the magnitude of the eddy heat fluxes at time T_E are small (Figure 5c).

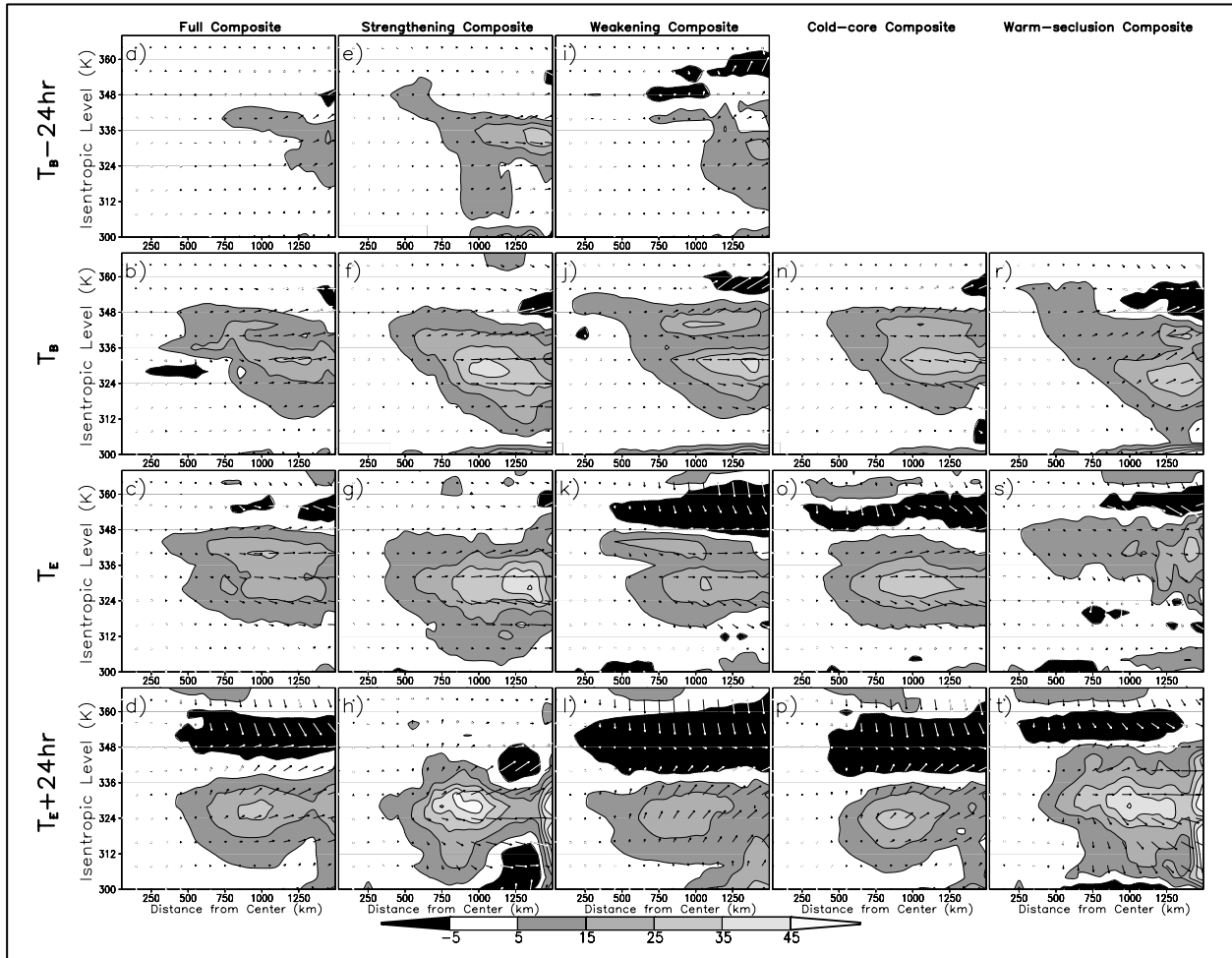


Figure 5: Cross sections ($r-\theta$) of Eliassen-Palm Flux vectors and their divergence (shaded; $10^5 \text{ Pa m}^2 \text{K}^{-1} \text{s}^{-2}$) for each subcomposite at four of the key ET benchmarks: $T_B-24\text{hr}$, T_B , T_E , and $T_E+24\text{hr}$. Radial component of the vector is the angular momentum flux, while the vertical component is the heat flux. Outward pointing arrows represent inward eddy angular momentum flux while downward-pointing arrows represent outward eddy heat flux. Method based on Molinari et al. (1995). Subcomposite fields were not calculated for $T_B-24\text{hr}$ for the cold-core and warm-seclusion subcomposites.

Molinari et al. (1995) found that in the trough-induced intensification of Hurricane Elena (1985), the eddy angular momentum forcing was maximized around 345K. The consequence of this forcing was to weaken the anticyclonic circulation aloft, decreasing the vertical wind shear and destroying the TC's thermal wind balance. In an attempt to regain thermal wind balance, the TC response is to produce a couplet of circulation centered on the eddy angular momentum forcing: direct below and indirect above, with enhanced inflow above and below and enhanced outflow in the region of the momentum flux forcing. This leads to adiabatic motion in the troposphere that restores thermal wind balance. Molinari et al. (1995) further argue that the adiabatic motion acts as a trigger to enhance the TC secondary circulation, increase convection and diabatic warming aloft, intensifying the storm.

In the case of the ET composite in Figure 5a-d, the eddy angular momentum forcing is centered considerably lower in the atmosphere (330-336K—approximately 500hPa), is also much broader in depth, and located at larger radii. With a deeper and lower layer of eddy momentum flux forcing, the response of the TC wind field will be to cyclonically accelerate the entire outer wind profile under the influence of the eddy angular momentum flux from the trough. In the lower troposphere the adiabatic response would be cooling at inner radii, while in the upper troposphere the adiabatic response would be cooling at larger radii. Given the convergent TC circulation in the lower troposphere, this adiabatic cooling would presumably drive frontogenesis, consistent with Harr and Elsberry (2000) and Harr et al. (2000). It is this adiabatic cooling that leads to the increase in the value of B in the cyclone phase space depiction. This is not to say that pre-existing frontal

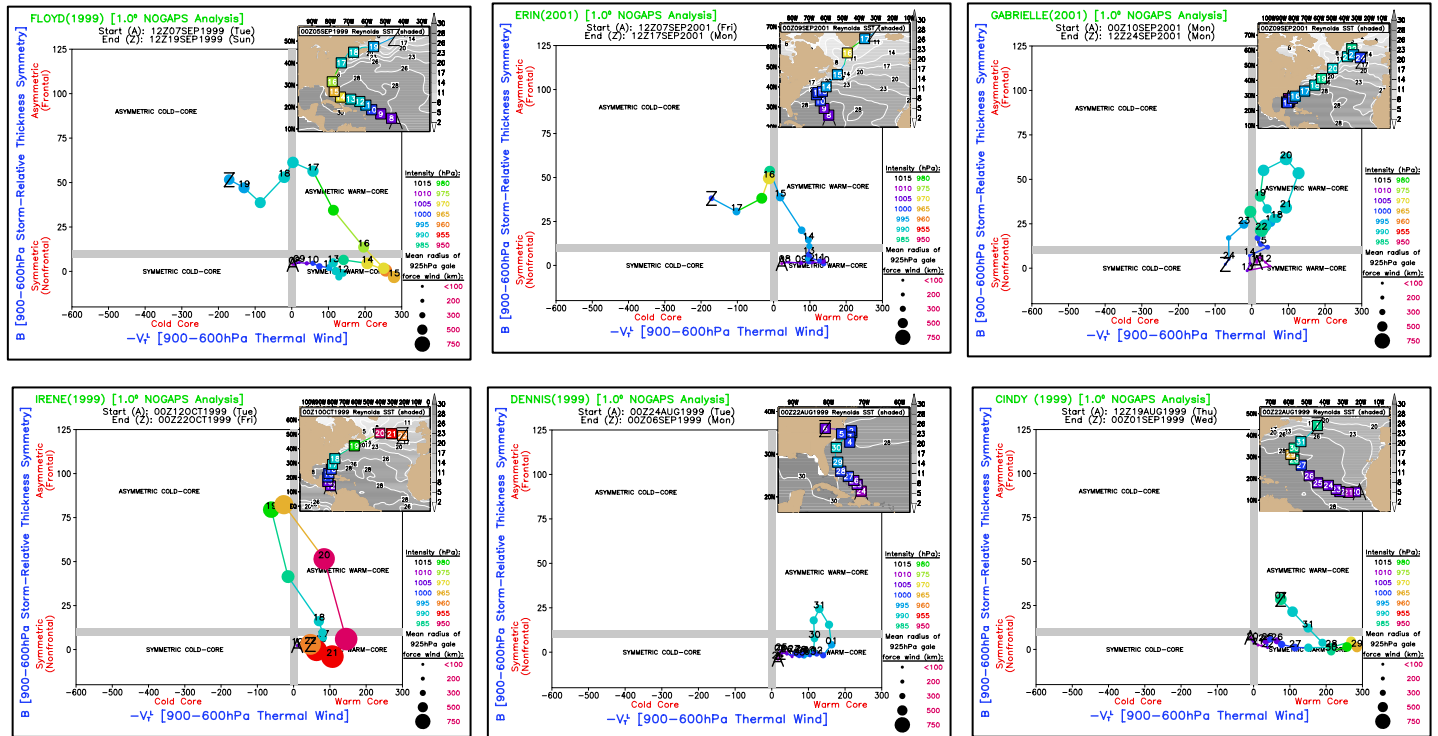


Figure 6: Examples of the variety of post-transition structural evolutions comprising the 34-member ensemble that lead to the dramatic increase in post-ET variability: a) Cold-core decay [Floyd 1999]. b) Cold-core intensification [Erin 2001]. c) Extended hybrid existence [Gabrielle 2001]. d) Warm-seclusion development [Irene 1999]. e) Halted ET and reacquired tropical structure [Dennis 1999]. f) Absorption by preexisting cyclone [Cindy 1999]. Only two dimensions (B vs. $-V_T^L$) of the cyclone phase space are shown.

zones cannot also accelerate or initiate the ET process; however, the composite mean of 34 cyclones argues that the adiabatic cooling response from the eddy angular momentum flux in the outer circulation far precedes it, when an upper atmospheric trough is present.

One day after transition (Figure 5d), we now see a classic eddy forcing pattern for an extratropical cyclone with strong inward eddy PV flux between 750 and 1000km, and outward eddy PV flux above 340K. The magnitudes of eddy heat and momentum fluxes have increased dramatically, with an intense direct circulation typical of an extratropical cyclone. The EP flux vectors above 350K are directed almost exclusively downward, suggesting the eddy heat flux is overwhelming the momentum flux at upper levels. This intense outward eddy heat flux is the result of the initially upright vortex tilting westward with height as it becomes baroclinic, such that the cyclone center is no longer aligned at all levels with the cylindrical coordinate used in the EP flux calculations. With the cylindrical coordinate system no longer collocated with the cyclone center aloft, the eddy heat flux is exaggerated with respect to the actual cyclone center.

4. FACTORS DISTINGUISHING TRANSITION EXTREMES

Although the mean cyclone evolution just examined is revealing, it fails to elucidate the variability that exists from case to case in the ET lifecycle. While variability in the hours leading up to the start of ET is relatively small, variability once ET has commenced increases dramatically. The CPS variability can be further characterized by examining the various cyclone phase space evolutions for representative members of the 34-cyclone composite (Figure 6). Hurricane Floyd (1999; Figure 10a) represents a case where the post-ET evolution is one of cold-core decay, while Hurricane Erin (2001; Figure 10b) represents a case where the post-ET evolution is one of cold-core intensification. While most TCs take less than 36h to complete the transition process (Evans and Hart 2003), occasionally the transition process can take several days. Hurricane Gabrielle (2001; Figure 10c) is one example of a slow transitioning TC. Occasionally, a transitioned TC can undergo warm-seclusion and rapid post-ET reintensification. In these cases, a pocket of warm air is trapped (secluded) in the center of the circulation (Shapiro and Keyser 1990). This structural change has very significant

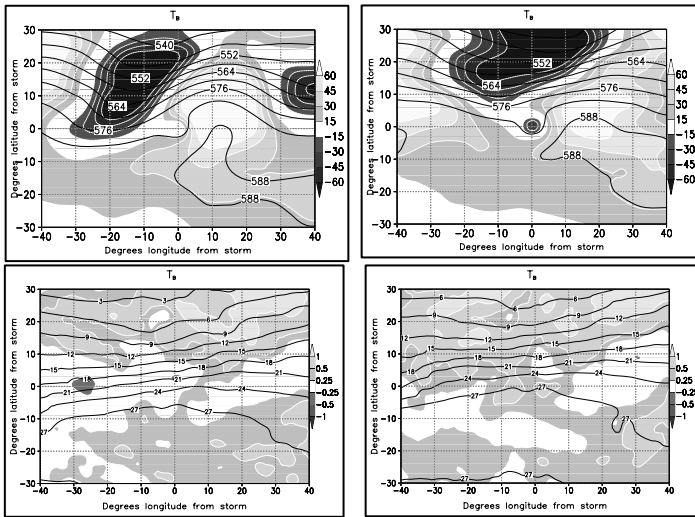


Figure 7: Comparison of the environments at T_B of cyclones that take 12h or less (left) and 48hr or more (right) to complete transition. a,b) 500hPa height (contour, dm) and anomaly from monthly mean (shaded, m). c,d) SST (contour, °C) and anomaly from weekly mean (shaded, °C).

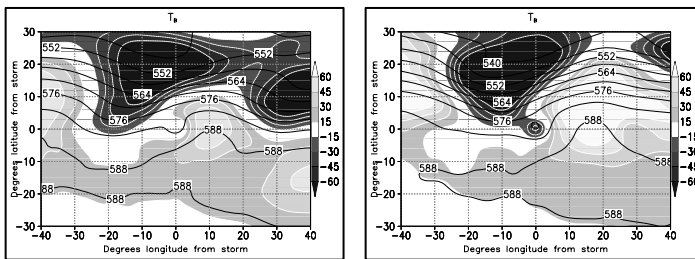


Figure 8: T_B subcomposites for post-ET: weakening (left) or strengthening (right). Weakening (strengthening) storms increase (decrease) in MSLP by at least 4hPa between T_E and T_E+24h . a,b) 500hPa height (contour) and anomaly from zonal mean (shaded).

implications that will be discussed. An example of such an evolution is Irene (1999; Figure 6d). Although not shown, a warm seclusion can occasionally lead to weakening, as happened with Earl (1998). Less frequently, a TC can begin ET, but not complete the process of transition, ultimately regaining tropical structure. In the case of Hurricane Dennis (1999; Figure 6e), the TC moved back equatorward into a region of decreasing shear and passed over the Gulf Stream, reversing the structural changes toward baroclinic development. Finally, a TC can begin the process of ET but be absorbed by a preexisting extratropical cyclone or be sheared apart before transition completes (e.g. Hurricane Cindy (1999); Figure 6f).

The nature of post-transition evolution is fundamentally key to the ultimate impact the cyclone will have on both marine and over-land interests. The radius of gale force winds (symbolized by the size of the circles along the CPS path) varies greatly in each of the cases shown in Figure 6, and even in the mean of each subcomposite type. Further, the intrinsic

predictability (whether physical or numerical) of the transitioning cyclone varies depending upon the evolution taken. Jones et al. (2003b) have shown that the global long-wave pattern predictability becomes dramatically decreased when a TC moves into the middle latitudes. Since numerical models often have difficulty handling the details of transition and post-transition evolution effectively, it would be helpful to determine and understand the patterns favorable for the various types of cyclone evolutions shown in Figure 6. To isolate these patterns responsible and to understand the environments determining ET evolution and post-ET intensity and structural change more fully, we next examine synoptic subcomposites for six sets of contrasting evolutions.

a. Rapid ($T_B \rightarrow T_E \leq 12hr$) versus slow ($T_B \rightarrow T_E \geq 48hr$) transitioning TCs

While the average length of time taken for ET to complete is approximately 30h (Evans and Hart 2003), there is considerable variability in the time taken to transition (Table 1). To understand the environments that distinguish rapid transitioning TCs (9 cases) from slow transitioning TCs (10 cases), composites of each group at T_B are examined (Figure 7).

Rapid transitioning TCs are associated with a higher amplitude trough than slow transitioning TCs (Figure 7). Thus, slow transitioning TCs are advected zonally across the Atlantic rather than meridionally. Further, slow transitioning TCs occur over SST about 3-4°C warmer than rapid transitioning TCs, and are 10hPa deeper than fast transitioning TCs at T_B (Table 1). It is noteworthy that the mean SST for slow transitioning TCs is 26.5°C, suggesting that, in the mean, the oceanic environment may still remain conducive to tropical development while ET is occurring. The highly amplified trough, typical of rapid transitioning TCs, steers the TC down the SST gradient; the weaker trough associated with slow transitioning TCs steers the TC roughly parallel to an SST isotherm. Should the unstable thermodynamic core coexist with SST of 26-27°C within a baroclinic environment, both modes of development are possible and would compete for structural change, delaying ET completion (Hart and Evans 2001).

In the mean, a rapid (slow) transitioning TC is also a smaller (larger) and weaker (stronger) TC on average (Table 1). This intensity differs by a full Saffir-Simpson category. Although requiring further study, it would seem that a smaller and weaker TC would be more prone to the shearing effects of a midlatitude trough, more rapidly removing the tropical aspects of the cyclone. It is noteworthy that there is no statistically significant difference in the mean latitude of slow vs. fast transitioning TCs

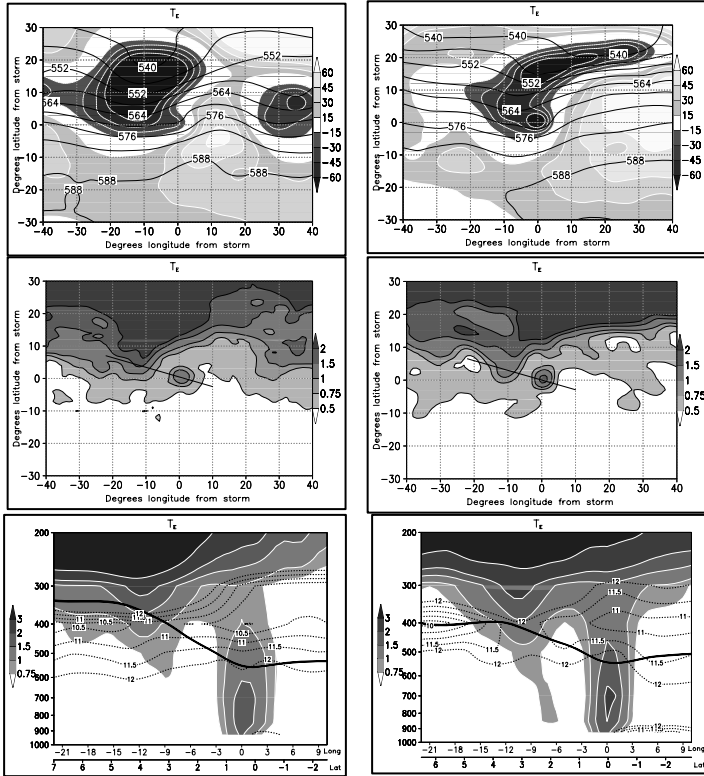


Figure 9: Synoptic environments at T_E that lead to left) cold-core evolution and right) warm-seclusion evolution after T_E . a,b) 500hPa height (contour, dm) and anomaly from monthly mean (shaded, m). c,d) 320K isentropic potential vorticity (shaded, PVU). e,f) Potential vorticity cross section along axis shown in c,d. (Table 1), arguing that the statistically significant size difference at T_B (Table 1) is not due to changes in coriolis during conservation of absolute angular momentum.

b. Discrimination of post-ET intensification from decay

Determination of whether a cyclone will undergo intensification or decay post-ET is critical to accurate forecasting of the storm-related weather at this stage. Post-ET intensity change is defined here as the change in minimum MSLP between T_E and T_E+24h . Intensification (decay) is defined as a 4hPa or larger magnitude decrease (increase) in minimum MSLP in this 24h period. Cases where the cyclone interacted with land during ET have been excluded to focus on the atmosphere pattern differences.

To focus on the precursor conditions leading to post-ET intensity change, subcomposites of the two groups of intensity change are produced for the time T_B (Figure 8). The orientation of the tilt of the 500hPa trough (Figure 8a,b) is the most striking distinction between these intensity subcomposites. For the post-ET intensifiers (weakeners), a negatively (positively) tilted 500hPa large-scale trough is advancing on the TC. Also noteworthy is that the

separation distance between the trough and TC varies considerably between the composites, with the post-ET intensifier have a much closer approach than the post-ET weakener. However, the number of cases in this sample (6) strongly argues for further investigation of this sensitivity. Indeed, two such cases preceding this study (Iris (1995) and Lili (1996)) do not conform to this result (Thorncroft and Jones 2000). A post-ET intensifying cyclone has an associated maximum of 850hPa equivalent potential temperature that extends 10° equatorward, while the post-ET weakeners are far more isolated from the tropical environment (Figure 8c,d). SST below an intensifying storm are $1-2^\circ\text{C}$ higher than below a weakening storm, but there is also a substantially increased gradient of SST below a strengthening storm. These results are all consistent with the idealized models favoring baroclinic growth (Charney 1947; Eady 1949), and reinforce the conclusion that the basic structure of both the TC and midlatitude trough play key roles in determining the nature of post-transition intensity change.

An even more striking comparison of the evolutions leading to post-ET weakening versus strengthening can be found in the time sequence of EP flux divergence for the mean atmosphere of the two subcomposites (Figure 5e-l). The post-ET strengthening subcomposite (which has a negatively tilted trough driving it; Figure 8b) is associated with significantly stronger eddy PV flux (from primarily inward transport of eddy angular momentum) at smaller radii than the post-ET weakening subcomposite (Figure 5i-l). The weakening subcomposite shows a maximum of eddy PV flux that contracts until T_E , after which it weakens and becomes less distinct. In contrast, the strengthening composite eddy PV flux undergoes a significant contraction and intensification between T_E and T_E+24h . This dramatic enhancement and contraction of the eddy PV flux maximum is made possible by the negative tilt of the synoptic-scale trough. The negative trough tilt both permits the TC to approach the trough to a much smaller distance, and also drives heat and momentum fluxes that amplify the trough itself, further increasing the eddy PV flux into the cyclone (Figure 5g,h).

c. Post-transition warm-seclusion from cold-core evolution

Shapiro and Keyser (1990) documented an extension to the fundamental cold-core lifecycle of extratropical cyclones. The development of a warm-seclusion within the center of extratropical cyclones can be achieved either as a precursor to, or as a result of, rapid intensification of extratropical cyclones (Hart 2003). The warm-core is typically restricted below 600hPa (Hart 2003), distinguishing the warm-

seclusion development from the deep warm-core development of TCs. Another distinctive factor is the dramatic expansion of gale force winds associated with warm seclusions. During a warm-seclusion, the strongest winds contract in radius while the radius of gale force winds expands. Thus, the development of a warm seclusion represents a dramatic increase in wind-driven threat through increases in both the area and magnitude of ocean-wave growth and land-surface damage potential. Essentially, the warm-seclusion process of an extratropical cyclone results in the combined threats of a cold-core cyclone (expanded area of strong winds) and TC (increased upper bound of destructive wind magnitude). As this type of development is often difficult to forecast numerically because of sensitivity to heating magnitude and distribution (Gyakum 1983a,b), it is critical to understand the precursor conditions that distinguish a future warm-seclusion from a conventional cold-core post-ET evolution (Figure 9). As not all warm-seclusions intensify (McTaggart-Cowan et al. 2001,2003), it is equally important to diagnose whether the warm-seclusion is a *response* to the intensification, or the *cause* of it.

The process of warm-seclusion is a classic case of scale-matching, aided by a narrowing of the approaching trough as in Molinari et al. (1995). As evidenced by the 500hPa analysis (Figure 9a,b) and the isentropic potential vorticity (Figure 9c-f), the scale of the midlatitude trough is key to determining the structural evolution of the cyclone after T_E . Cyclones that undergo a warm-seclusion after T_E interact with a trough that is considerably narrower in horizontal scale, but more extensive in vertical scale, than a cyclone that remains cold-core after T_E . Thus, for a future warm-seclusion the horizontal and vertical scale of the trough is a closer match to that of the tropical storm (Figure 9c vs. d) and the trough signature itself also extends much lower into the troposphere (Figure 9e vs. 9f) than for a post-ET cold-core development, consistent with Molinari et al. (1995) and Hanley et al. (2001). Indeed, a TC that undergoes a warm-seclusion is on average 50% larger than a TC that remains cold-core after transition (Table 1). Thus, the scale matching is achieved through an above-average TC size along with a narrowing of the trough.

As was the case in the previous subcomposite intercomparison, the Eliassen-Palm flux vector comparisons for the cold-core vs. warm-seclusion subcomposites are insightful for explaining the details and sensitivity of the interaction (Figure 5n-t). In particular, while the cold-core composite is unremarkable, at the end of transition (Figure 5o), the warm-seclusion subcomposite bears considerable resemblance to the trough interaction case of Elena

(Figure 5s; compare with Molinari et al. 1995 Figure 3c,d). While all other cross sections in Figure 5 show a level of maximum eddy PV flux below 330K, Figure 5s alone has a level of maximum PV flux of 340-345K, approximately the same as for Elena (1985). As Molinari et al. (1995) argued in the case of Elena, the narrowing of the trough as it approaches the TC leads to eddy angular momentum flux that is focused on the outflow anticyclone of the TC (due to Rossby depth reduction). The (in)direct circulation (above) below 345K regains thermal wind balance through adiabatic motion. As a response to this motion, the secondary circulation of the TC is enhanced and there is a short-term intensification. This begs the question, then, of how the cyclone response is different if the cyclone is transitioning to cold-core.

Figure 5r suggests that the start of transition for a future warm-seclusion is not unique. There is a deep layer of eddy PV flux that is maximized in the middle troposphere (325K). The cyclone responds to this forcing as described earlier. Based upon Figure 5r, it would appear that the scale of the trough does not play a factor while the trough is still beyond the extreme outer edge of the TC circulation (Figure 9d). However, instead of continuing to deepen and strengthen as was the case in the other subcomposites (Figure 5c,g,k,o), the region of eddy PV flux suddenly contracts and moves upward – in response to the narrowing of the trough (Figure 9d,f). Thus, in the middle of transition, the TC is now in an environment for an Elena-type rapid intensification. With the sudden scale decrease and elevation of the eddy PV flux, a much more focused eddy momentum response occurs, as did with Elena (Molinari et al. 1995). A direct (enhanced secondary) circulation forms within the entire troposphere below 345K, causing dramatically enhanced low-level inflow, adiabatic ascent at inner radii, and outflow at the 345K level, to restore thermal wind balance. The cyclone response as a consequence of this eddy forcing change during transition is seemingly the generation of a warm-seclusion around or after T_E+24hr .

One day following transition, this rapid contraction is illustrated in Figure 5t, with the deepest layer of inward eddy PV flux of any of the panels on Figure 5. The deep layer of downward EP flux vector in Figure 5t is indicative of the formation of the warm seclusion, since the vector direction indicates intense heat flux outward from the center of the vertically upright lower tropospheric vortex. Finally, it is worthwhile to note that there are no significant differences in the SST field (Figure 9i,j) beneath the cyclone that becomes a warm-seclusion and the cyclone that remains cold-core.

| | Number of cases | Mean Latitude at T_B | Mean Longitude at T_B | Mean NHC Best-Track Intensity at T_B (hPa) | Mean NHC mean radius of gale force winds at T_B (km) |
|-------------------------------------|-----------------|------------------------|-------------------------|--|--|
| Entire composite | 34 | 34.3 (5.8) | -65.6 (16.1) | 982.8 (15.3) | 211.8 (97.4) |
| Slow transitioning TC subcomposite | 9 | 33.0 (6.2) | -66.5 (14.4) | 972.8 (16.2) | 263.0 (59.7) |
| Fast transitioning TC subcomposite | 10 | 36.1 (5.0) | -67.2 (11.4) | 987.7 (13.9) | 184.3 (115.8) |
| Post-ET Intensifier subcomposite | 6 | 37.0 (1.8) | -59.8 (7.3) | 980.6 (15.1) | 255.3 (107.2) |
| Post-ET weakener subcomposite | 11 | 36.2 (4.9) | -63.0 (15.8) | 982.6 (11.5) | 194.2 (90.2) |
| Post-ET warm-seclusion subcomposite | 6 | 32.5 (6.7) | -72.7 (15.5) | 982.0 (13.5) | 259.8 (64.0) |
| Post-ET cold-core subcomposite | 15 | 36.2 (4.6) | -57.9 (15.2) | 986.5 (13.2) | 171.1 (96.6) |

Table 1: Mean statistics on each of the composites. Standard deviation is denoted in parentheses. Statistically significant departures within each sub-composite (slow vs. fast, intensifier vs. weakener, and warm-seclusion vs. cold-core) to 90% (95%) confidence using a t-test, are shaded in light (dark) gray. Note that the subcomposites are not independent. Thus a single storm may contribute, for example, to the post-ET intensifier *and* the warm seclusion subcomposites.

5. CONCLUSIONS

The evolution of a TC from a warm-core vortex to a cold-core vortex is largely driven by the eddy angular momentum flux of the trough, rather than the eddy heat flux associated with the trough. The response of the transitioning cyclone to the tropospheric-deep PV forcing is to produce adiabatic ascent and cooling inward and beneath the region of the eddy forcing to restore thermal wind balance. In the case of ET, the eddy PV flux forcing is maximized considerably lower in the atmosphere, and spread over much greater depth, than in the case of rapid intensification of a hurricane (e.g. Elena 1985; Molinari et al. 1995). Only after ET has completed (T_E in the cyclone phase space) is the eddy heat flux forcing diagnosed as significant, consistent with Harr et al. (2000).

The nature of the ET evolution and intensity change is sensitive to the scales of interaction of the trough and TC, in both space and time. The tilt and scale of the interacting trough play statistically significant roles throughout the entire evolution, while the SST appears to play an important role only until transition is completed. A TC undergoes rapid ET if the long wave pattern is highly meridional, the SST are several degrees below 27°C with a large SST gradient, and the TC is significantly smaller and weaker than average at the beginning of ET (Table 1). A TC undergoes slow transition (and has an extended hybrid phase) if the long wave pattern is

more zonal, the SST beneath the TC are closer to 27°C , and the TC is significantly larger and stronger than average; this combination of environmental forcings continues to support tropical development ($\text{SST} \sim 27^\circ\text{C}$) at the same time as ET is occurring.

Once transition completes (T_E), an ET-TC will undergo post-transition intensification if the interacting trough is negatively tilted and the remnant TC is intense. If the remnant TC is weak or the interacting trough is positively tilted, the ET-TC will weaken. In the 24-48hr following transition, approximately 70% of ET cases result in cold-core evolutions while 30% result in warm seclusions. If the interacting trough acquires a size that permits scale matching with the remnant TC (minimizes the trough scale), then a warm-seclusion (cold-core cyclone) results. A warm-seclusion occurs as a consequence of the eddy PV flux from the trough contracting to the outflow layer of the transitioning TC, consistent with the Molinari et al. (1995) model for Elena (1985).

The results presented here suggest sources of the abnormally low predictability of the long-wave pattern during ET events. Differences in TC intensity, depth, trough tilt or scale, or latitude of transition (SST) can lead to extreme variability in the forecast evolution of the post-ET cyclone *and* the interacting long-wave pattern. With numerical models initializing TCs often 30-50mb too weak, it is not at all surprising to find the great disparity of ET

structural forecasts today (<http://moe.met.fsu.edu/cyclonephase>; Hart and Evans 2003; Evans and Arnott 2004). The results of this research argue that great care must be taken when initializing numerical models around the time of an ET event. Further, it is important to understand how well the evolving tropical storm structure is initialized in the operational models, including the use of synthetic observations (Goerss and Jeffries 1994; Kurihara et al. 1998; Liu et al. 2000).

In addition to the tropical vortex, all of these evolutions depend upon the scale and timing of the interacting trough, which also may not be sufficiently well analyzed, especially over the oceans. Thus, improved analysis of areas producing sensitivity to ET and post-ET track and intensity forecasts should be a priority to improve mid-latitude forecasts (Jones et al. 2003b). Further, with 3-5 day official track forecast errors by NHC averaging 300-500km (and recurving storms having even larger errors on average), one can readily see how even average track forecast error in a numerical forecast can lead to a dramatic change in the simulated TC-trough interaction and thus post-ET evolution.

6. ACKNOWLEDGMENTS

The first author was funded by a UCAR Visiting Scientist Position during the early part of this research, and is grateful to UCAR, NCEP, and in particular Steve Lord and Naomi Surgi of NCEP/EMC for making this support possible. The first author was also funded by a Florida State University CRC FYAP grant during the second half of this research. The second author was supported by the National Science Foundation under Grant ATM-0351926. The third author was supported by an AMS/ONR Fellowship. The authors are grateful to these organizations for their support.

The NOGAPS analysis and forecast data was provided by Mike Fiorino of Lawrence Livermore National Lab. Figures for this paper were created using the GrADS software package from COLA/IGES. The research has greatly benefited from discussions with Eyad Attalah of McGill University, Lance Bosart of SUNY Albany, and Ryan N. Maue of Florida State University.

7. REFERENCES

Arnott, J. M., J. L. Evans, and F. Chiaromonte, 2004: Characterization of ET using cluster analysis. *Mon. Wea. Rev.*, **132**, 2916-2937.

Bosart, L. F., E. H. Atallah, and J.E. Molinari, 2001: The quantitative precipitation forecast problem associated with landfalling and transitioning tropical cyclones. *Preprints, Symposium on Precipitation Extremes, 81st Annual Meeting of the American Meteorological Society*, Albuquerque, NM, January 2001.

Charney, J. G., 1947: The dynamics of long waves in a baroclinic westerly current. *J. Meteor.*, **4**, 135-162.

Eady, E. T., 1949: Long waves and cyclone waves. *Tellus*, **1**, 33-52.

Evans, J. L., and J. M. Arnott, 2004: Analysis of operational model forecast trends in ET storm structure. *26th AMS Tropical Meteorology and Tropical Cyclones Conference*, Miami Beach, FL, 3-7 May 2004.

Evans, J. L., and R. E. Hart, 2003: Objective indicators of the onset and completion of ET for Atlantic tropical cyclones. *Mon. Wea. Rev.*, **131**, 909-925.

Goerss, J.S. and R. A. Jeffries, 1994: Assimilation of Synthetic Tropical Cyclone Observations into the Navy Operational Global Atmospheric Prediction System. *Weather and Forecasting*, **9**, 557-576.

Hanley, D., J. Molinari, and D. Keyser, 2001: A Composite Study of the Interactions between Tropical Cyclones and Upper-Tropospheric Troughs. *Mon. Wea. Rev.*, **129**, 2570-2584.

Harr, P., and R. L. Elsberry, 2000: ET of Tropical Cyclones over the Western North Pacific. Part I: Evolution of Structural Characteristics during the Transition Process. *Mon. Wea. Rev.*, **128**, 2613-2633.

Harr, P., R. L. Elsberry and T. Hogan, 2000: ET of tropical cyclones over the western North Pacific. Part II: The impact of midlatitude circulation characteristics. *Mon. Wea. Rev.*, **128**, 2634-2653.

Hart, R. E., 2003: A cyclone phase space derived from thermal wind and thermal asymmetry. *Mon. Wea. Rev.*, **131**, 585-616.

Hogan, T. F., and T. E. Rosmond, 1991: The description of the Navy Operational Global Atmospheric Prediction System's spectral forecast model. *Mon. Wea. Rev.*, **119**, 1786-1815.

Jones, S. C., and coauthors, 2003a: The ET of Tropical Cyclones: Forecast Challenges, Current Understanding, and Future Directions. *Wea. and Fore.*, **18**, 1052-1092.

Jones, S., C. Velden, S. Aberson, J. Abraham, P. Harr., 2003b: ET, Thorpex, and the North Atlantic TrEC. *Proceedings, 2nd International Workshop on ET*. Halifax, NS, November 2003.

Kanamitsu, M., 1989: Description of the NMC global data assimilation and forecast system. *Wea. Forec.*, **4**, 335-342.

Kurihara, Y., R. E. Tuleya and M. A. Bender, 1998: The GFDL Hurricane Prediction System and Its Performance in the 1995 Hurricane Season. *Mon. Wea. Rev.*, **126**, 1306-1322.

Klein, P., P. Harr and R. L. Elsberry, 2000: ET of western North Pacific tropical cyclones: An overview and conceptual model of the transformation stage. *Wea. Forc.*, **15**, 373-396.

Liu, Q., T. Marchok, H-L. Pan, M. Bender, and S. Lord, 2000. Improvements in hurricane initialization and forecasting at NCEP with global and regional (GFDL) models. *Technical Procedures Bulletin No. 472*. Available at: <http://205.156.54.206/om/tpb/472.htm> or from NOAA/NWS Silver Spring, MD.

McTaggart-Cowan, R., J. R. Gyakum, and M.K. Yau, 2001: Sensitivity Testing of ETs Using Potential Vorticity Inversions to Modify Initial Conditions: Hurricane Earl Case Study. *Mon. Wea. Rev.*, **129**, 1617-1636.

McTaggart-Cowan, R., J.R. Gyakum, and M.K. Yau, 2003: The Influence of the Downstream State on ET: Hurricane Earl (1998) Case Study. *MWR.*, **131**, 1910-1929.

McTaggart-Cowan, R., J.R. Gyakum, M.K. Yau, 2004: The Impact of Tropical Remnants on Extratropical Cyclogenesis: Case Study of Hurricanes Danielle and Earl (1998). *Mon. Wea. Rev.*, **132**, 1933-1951.

Molinari, J., S. Skubis, and D. Vollaro, 1995: External influences on Hurricane Intensity. Part III: Potential Vorticity Structure. *Mon. Wea. Rev.*, **52**, 3593-3606.

Thorncroft, C., and S. C. Jones, 2000: The ET of hurricanes Felix and Iris in 1995. *Mon. Wea. Rev.*, **128**, 947-972.